

SMAD signaling promotes melanoma metastasis independently of phenotype switching

Eylül Tuncer¹, Raquel R. Calçada¹, Daniel Zingg¹, Sandra Varum¹, Phil Cheng², Sandra N. Freiburger², Chu-Xia Deng³, Ingo Kleiter⁴, Mitchell P. Levesque², Reinhard Dummer², and Lukas Sommer

Supplemental Experimental Procedures

Supplemental Table 1

Supplemental Table 2

Supplemental Table 3

Supplemental Table 4

Supplemental Table 5

Supplemental Table 6

Supplemental Table 7

Supplemental Table 8

Supplemental Table 9

Supplemental Table 10

Supplemental References

Supplemental Figure Legends

Supplemental Figure 1

Supplemental Figure 2

Supplemental Figure 3

Supplemental Figure 4

Supplemental Figure 5

Supplemental Figure 6

Supplemental Figure 7

Supplemental Experimental Procedures

Administration of Tamoxifen and Analysis of Mice

Transgenic lines were crossed to the Rosa26 Cre reporter strain (*R26R*), which has a ubiquitously expressed transgene containing a STOP cassette flanked by loxP sites followed by the *LacZ* gene. The resulting mice *Tyr::Nras^{Q61K} Ink4a^{-/-} Smad4^{lox/lox} R26R::LacZ* mice, *Tyr::Nras^{Q61K} Ink4a^{-/-} Smad4^{lox/wt} Tyr::CreERT² R26R::LacZ* mice (control groups) and *Tyr::Nras^{Q61K} Ink4a^{-/-} Smad4^{lox/lox} Tyr::CreERT² R26R::LacZ* mice (experimental group) were subjected to treatment with tamoxifen (T5648, Sigma Aldrich, Missouri, USA), which was diluted in ethanol and sunflower oil (1:9 ratio). Conditional ablation of *Smad4* as well as *Smad7* was achieved by intraperitoneal injections of tamoxifen (100 μ l, 1 mg d⁻¹ for 5 days) into 4-week-old mice and 4-months-old mice. Topical administration of 4-hydroxytamoxifen (4-OHT) (H7904, 98% Z-isomer, Sigma Aldrich, Missouri, USA) was performed by preparing a 50 mg/ml (130 mM) solution of 4-OHT in dimethyl sulfoxide; DMSO (M810802, Sigma Aldrich, USA) 4-week-old mice were treated with Veet cream to remove hair from 2 x 2 cm patch of skin on the dorsal flank. After the area was dried and topical administration of 50 mg/ml stock solution in DMSO was diluted into 100% ethanol and freshly applied (1 ml, for 3 days). Upon intraperitoneal (IP) Tamoxifen injections or topical 4-OHT administration, mice were monitored for tumor numbers and development. In combination with staining for the *R26R::LacZ* Cre-reporter allele, the macroscopic skin phenotype was analyzed histologically. Mice were examined regularly and sacrificed at an endpoint defined by adverse clinical symptoms including skin tumor size ($\emptyset > 2$ mm), weight loss, or hunched back.

Quantification of Skin Melanomas and Metastases

At day of sacrifice, skin melanoma numbers were counted. Non-recombined tumors were excluded for statistical analysis. Both in conditional *Smad4* and *Smad7* knockout mice (cKO), whole mount X-Gal (Invitrogen, California, USA) staining was used to assess the recombined tumors. Quantification of the percentage of mice bearing macro-metastases in each organ including lung, liver and spleen were visually examined under the binocular at necropsy and calculated by counting pigmented lesions at the organ surface. Affected lymph nodes (accessory axillary, proper axillary, sciatic and subiliac lymph nodes) were further assessed by immunohistostaining. PAX3, DCT and HMB-45 positivity was used to detect melanoma cells on lung, liver, and spleen on histological sections.

Immunofluorescent Labeling

Cells were grown on cover slips, ethanol-fixed, and subjected to immunofluorescent labelling using primary antibodies (Supplemental Table 8) in blocking buffer (1% BSA in PBS and 0.05% Tween) overnight at 4°C and secondary antibodies (Supplemental Table 8 for 1h at room temperature. Nuclei were stained with Hoechst 33342 (14533, Sigma-Aldrich, USA), and cells were recorded with a DMI 6000B microscope (Leica).

Hair Cycle Staging, Plucking

Morphogenetic and adult hairs were staged according to literature (1, 2). Plucking was performed to synchronize adult hairs. Briefly, mice were anesthetized, and hairs were removed in a 3 cm × 3 cm region on the back skin at every telogen stage. Hairs within this region were allowed to regenerate for 28 days after plucking procedure. TM was dissolved in corn oil or a

combination of ethanol and sunflower oil. TM treatment was performed by IP injection of adults with *Smad4^{lox/lox} Tyr::CreERT² R26R::LacZ* genotype (experimental group). Control group harbored the same genotype and was not received any TM.

Histologic Analysis and Immunohistochemistry

Mice were sacrificed by CO₂ inhalation. Samples were fixed in 4% (w/v) paraformaldehyde overnight. To achieve whole mount X-Gal staining, samples were fixed in 4% paraformaldehyde for only 20 min and subjected to X-Gal staining. Sections (5 μm) were stained with H&E, and serial sections were used for immunohistochemical analysis. Sections were deparaffinized and subjected to an antigen retrieval step using citrate buffer (S2369, Dako) (Rapid Microwave Histoprocessor, Milestone). Primary antibodies (Supplemental Table 8) were applied in blocking buffer (1% BSA in PBS and 0.05% Triton X-100) overnight at 4°C and visualized using secondary antibodies (Supplemental Table 8) in blocking buffer for 1h at room temperature. Antigen retrieval with heating in citric acid (pH 6.0) was done. Heavily pigmented skin slides were pre-treated with 0.1% KMnO₄ for 20 min followed by 0.5% oxalic acid for 12 min to increase the solution permeabilization. For visualization of β-Galactosidase and phospho-SMADs, biotin anti-chicken and biotin anti-rabbit secondary antibodies was combined with further signal amplification using horse radish peroxidase–streptavidin and the TSA Plus Cy3 Kit (1:50, NEL744001KT, PerkinElmer) according to manufacturers' protocol. Subsequently, nuclei were stained with Hoechst 33342 (14533, Sigma-Aldrich) slides were mounted with Fluorescent Mounting Medium (S3023, Dako). Immunohistochemical / fluorescent sections were analyzed using either a Mirax Midi Slide Scanner (Zeiss) or a DMI 6000B microscope (Leica). Recombination efficiency of the Rosa26 allele was examined in mice by counting the β-Gal fluorescent cells of each tumor and dividing by the total number of DAPI-positive cells. Analysis of metastases was performed by counting distinct melanoma markers in each lesion (in sections

from each level throughout the organ). Lung, spleen and liver metastases were analyzed based on the number of Pax3, Dct fluorescent cells. Groupings included single (1 cell), micro (11–100 cells), and macro (> 100 cells).

Analysis of Proliferation and Apoptosis

To study tumor proliferation index, we investigated the incorporation of the thymidine analog 5-ethynyl-2'-deoxyuridine (EdU). Prior to sacrifice under isoflurane anaesthesia, mice were injected IP with 50 mg EdU/kg body weight. EdU was immunohistochemically on formalin-fixed and paraffin-embedded sections according to the manufacturer's guidelines. (Click-iT® EdU Alexa Fluor® 488 Imaging Kit, C310337, Invitrogen, USA). Cell proliferation was also assessed by Ki67 immunostaining. To quantify cells undergoing apoptosis, cleaved caspase-3 staining was used (see Histologic Analysis). Ten high-power fields (40 magnification) from at least 3 independent mice were counted for positive staining. Quantitative analysis was performed by counting cells in 10 independent high-power fields (40×) per age-matched tissue section from six mice per group.

Correlation Analysis

Melanoma cell cultures were established from surplus material from primary cutaneous melanoma and melanoma metastases removed by surgery as previously described (3) This was performed at Dermatology Department of University of Zurich. Cell lines were correlated to their high SOX10 and high MITF expression as proliferative and high WNT5A high ZEB1 and SOX9 expression as invasive. Pearson's product moment correlation (r) was calculated for each gene expression values across all patient derived human melanoma cell lines. P-value was determined from the t statistic calculated from R value.

Cell Growth, Cell Cycle Analysis and Ligand Treatments

The 501Mel cell line was obtained from the ATCC collection. The 501Mel cell line carries *BRAF*^{V600E} mutation. M010817 cell line were described previously (4). The M010817 cell line has *NRAS*^{Q61R} mutation (*BRAF* not mutated). Primary cells derived from *Tyr::Nras*^{Q61K} *Ink4a*^{-/-} induced tumors were cultured as previously specified (5). Cells were grown in RPMI-1640 medium supplemented with 10% FCS and 4 mM L-glutamine. Ligand treatment experiments were studied in serum-starved medium (0.5% FCS) (24 hours starved before ligand treatment). The effect of ligands on cell phenotype was determined by continuously adding human recombinant ligands that are indicated Supplemental Table 10 for 72 hours to cell monolayers at 70% confluency. To establish growth curves, cell counts were measured daily starting 12 h after transfection. For cell cycle analysis, the Click-iT EdU Alexa Fluor 647 Flow Cytometry Assay Kit (Invitrogen) was used. Cells were labelled with PI according to the manufacturer's protocol and the DNA content was measured using a BD FACS Canto II flow cytometer (BD Biosciences) and BD FACS Diva software (BD Biosciences).

RNA Interference

Silencing RNA (siRNA) transfection of human melanoma cells was carried out using jet PRIME siRNA Transfection Reagent (114-07, Polypus Transfection) solution according to the manufacturer's protocol. To achieve gene specific knockdown of SMAD4 and SMAD7, human melanoma cells were transfected with siRNA (25nM) (Invitrogen) 72 hours before RNA and protein isolation (Supplemental Table 9). As control, scrambled siRNAs with similar guanine cytosine (GC) content were also purchased from Invitrogen and used as negative controls. We confirmed the specificity of these sequences in BLAST. Growth medium was exchanged after 24h and cells were subjected to further assays.

Quantitative RT-PCR and RNA Sequencing

Total RNA was prepared using RNeasy Mini Kit (74104, Qiagen) and the RNase-Free DNase Set (79254, Qiagen) according to manufacturer's guidelines, reverse transcribed with Maxima First Strand cDNA Synthesis Kit (K1641, Thermo Scientific) followed by an RNase H (EN0202, Thermo Scientific) digestion step. Real-time quantitative PCR (qPCR) was performed on a LightCycler 480 System (Roche) using LightCycler 480 SYBR Green I Master (4707516001, Roche). Control of genomic contamination was measured for each sample by performing the same procedure with or without reverse transcriptase. Primers used mentioned in (Supplemental Table 9). Relative quantitative RNA was normalized using the housekeeping genes *β-actin* and *Gapdh*. The entire procedure was repeated in three biologically independent samples. Results were presented as the fold change over controls isolated from the same experiments. Fold induction was calculated using the comparative Ct method (DDCt). Total RNA obtained from 3 control and 3 siRNA mediated knockdown samples. Sample quality check was done using Bio-Analyzer. Samples were subjected to sequencing on Illumina Hiseq platform at the Functional Genomics Center Zurich (<http://www.fgcz.ch/>). Differential gene expression analysis was performed using a minimum fold change of 1.5 and a False Discovery Rate inferior to 0.05. Gene ontology network analysis was performed with ClueGO (Version 2.3.2) and Cytoscape (Version 3.4.0). Clusters with less than 10 nodes were omitted.

Protein Isolation and Western Blotting

Cells were lysed in RIPA buffer (89900, Thermo Scientific) including Halt Phosphatase and Protease Inhibitor Cocktail (78420, 87786, Thermo Scientific). SDS-PAGE was carried out with 20 µg of whole-cell protein lysate using 4–20% Mini-PROTEAN TGX Gels (456–1094, Bio Rad). The gels were blotted onto nitrocellulose membrane and blocked for 1h in Odyssey blocking

buffer (927-40000, LI-COR Biosciences). Primary antibodies (Supplemental Table 8) were applied in blocking buffer overnight at 4°C and visualized using secondary antibodies (Supplemental Table 8) for 45 min at room temperature. Blots were scanned and quantified with an Odyssey imaging system (LI-COR Biosciences). Quantified band intensities were normalized using either β -Actin or α -Tubulin as housekeeping protein.

TCGA Analysis

The RNA-seq and clinical data sets for skin cutaneous melanoma were downloaded on April 2016 from TCGA (<http://cancergenome.nih.gov/>). Normalized reads from the level 3 RNA-seq data were used for analysis. Specimens with top and bottom transcript levels for a gene of interest were used for analysis. Patient numbers were gradually increased from a minimum of top and bottom 11% (50 out of 470) to a maximum of top and bottom 11 % (50 out of 470) to optimize potential segregation of Kaplan–Meier curves.

Attachment Assay Using Fibronectin-Coated Plates

Six well plates were coated with 1.25 μ g/mL of fibronectin (F1141-5MG, Sigma) in PBS overnight at 4°C. Wells coated with bovine serum albumin served as negative controls. 1×10^4 cells were seeded in each well at 37°C. After ligand treatment, suspension cells were collected and were seeded in each fibronectin-coated well at 37°C. Unattached cells were discarded, and the attached cells were gently washed with PBS. Cells were fixed with 1% formaldehyde for 10 min and stained with 0.5% crystal violet for 30 min and solubilized with methanol. The area was calculated using Cell Profiler Program.

Analytical FACS

Single-cell suspensions of each treatment were pulsed with EdU and stained with primary and fluorochrome-conjugated secondary antibodies are listed in Supplemental Table 8. Intracellular MITF staining was performed following live cell AXL staining. Cells were detected by BD FACS Canto II flow cytometer (BD Biosciences) and analyzed with BD FACS Diva software (BD Biosciences).

Cell Sorting and Boyden Chamber Invasion Assay

Cells were transfected with siRNAs and cultured for 2 days with various factors using the same concentration as reported. After 48 hours of treatment, cells were harvested for flow sorting. For AXL flow sorting, cells were first washed with warm PBS, followed by an addition of 10mM EDTA to detach from flask. Cells were resuspended in cold PBS 2% FBS and kept on ice. Cells were counted, and 1,000,000 cells were transferred to 15 ml conical tubes (Falcon), spin down and resuspended in 100 μ l of cold PBS 2% FBS alone (negative control) or with AXL antibody. Cells were incubated on ice for 30 min, then washed twice with cold PBS 2% FBS. Cells were pelleted and resuspended in 100 μ l PBS 2% with Alexa 488-conjugated antibody. Samples were acquired with a BD Aria III 5L flow cytometer (BD Biosciences). First, doublets were excluded based on forward and sideward scatter, then we gated on viable cells and sorted single cells (AXL⁺ or AXL⁻). Data was analyzed using FACS Diva Version 6.2 using viable cells only and gates for AXL positivity were set using the unstained and secondary antibody only control. Subsequently Boyden Chamber invasion assays were done according to manufacturer's protocol. Briefly, 300,000 cells were subjected to matrigel-coated well inserts (354480, BD Biosciences) in empty medium (0% FCS and 0% L-Glutamine). Growth medium was used as chemoattractant for 24 h. Transvaded cells were 4% buffered formaldehyde fixed and visualized

using Hoechst 33342. Membranes were mounted to glass slides, and cell numbers were quantified using a DMI 6000B microscope and CellProfiler version 3.0.

Supplemental Table 1. GO Process

NODE	GOID	GO Term	P-Value	% Genes	Nr. Genes
1	GO:0092561	DNA-dependent DNA replication	130.0E-6	19.11	30.00
2	GO:0092562	DNA replication	13.0E-9	17.27	57.00
3	GO:0006259	DNA metabolic process	1.3E-3	10.37	107.00
4	GO:0044774	DNA replication initiation	550.0E-6	32.56	14.00
5	GO:0044765	Regulation of transcription involved in G1/S	1.2E-3	39.29	11.00
6	GO:0044774	G1/S transition of mitotic cell cycle	19.0E-6	16.80	42.00
7	GO:0044773	cell cycle G1/S phase transition	25.0E-6	16.41	43.00
8	GO:0098778	cell cycle phase transition	1.1E-3	11.99	68.00
9	GO:9087689	mitotic cell cycle phase transition	890.0E-6	12.24	66.00
10	GO:8976810	mitotic cell cycle process	4.1E-12	13.40	126.00
11	GO:0000278	mitotic cell cycle	2.0E-12	13.06	135.00
12	GO:0051726	regulation of cell cycle	11.0E-12	12.80	135.00
13	GO:0007346	regulation of mitotic cell cycle	32.0E-3	11.43	59.00
15	GO:0045786	negative regulation of cell cycle	14.0E-9	14.44	80.00
16	GO:0000075	cell cycle checkpoint	430.0E-9	18.15	45.00
17	GO:0031570	DNA integrity checkpoint	7.7E-3	16.20	29.00
18	GO:0007049	cell cycle	1.9E-15	11.72	211.00
19	GO:0007067	mitotic nuclear division	60.0E-9	15.07	69.00
20	GO:0022402	cell cycle process	100.0E-12	11.69	160.00
21	GO:0000280	nuclear division	450.0E-9	13.41	81.00
22	GO:0007088	regulation of mitotic nuclear division	290.0E-6	19.31	28.00
23	GO:0051301	cell division	41.0E-6	12.63	75.00
25	GO:0051276	chromosome organization	340.0E-6	11.84	78.00
26	GO:0071103	DNA conformation change	14.0E-3	13.78	39.00
27	GO:0000070	mitotic sister chromatid segregation	27.0E-3	16.78	24.00
28	GO:0007059	chromosome segregation	49.0E-6	14.78	51.00
29	GO:0044427	chromosomal part	15.0E-3	10.40	88.00
30	GO:0051783	regulation of nuclear division	36.0E-6	18.97	33.00
31	GO:0005694	chromosome	4.2E-3	10.33	99.00
32	GO:0051304	chromosome separation	44.0E-3	21.05	16.00
33	GO:0098609	cell-cell adhesion	14.0E-3	9.65	117.00
34	GO:0030155	regulation of cell adhesion	49.0E-3	10.60	73.00
35	GO:0050865	regulation of cell activation	6.3E-3	11.76	64.00
36	GO:0001775	cell activation	6.4E-6	11.42	110.00
37	GO:0045321	leukocyte activation	1.7E-3	11.01	87.00
38	GO:0098602	single organism cell adhesion	18.0E-3	10.40	86.00
39	GO:0016337	single organismal cell-cell adhesion	24.0E-3	10.53	81.00
40	GO:0002682	regulation of immune system process	12.0E-3	9.37	136.00
41	GO:0051240	positive regulation of multicellular process	5.8E-6	10.28	155.00
42	GO:0051094	positive regulation of developmental process	40.0E-6	10.49	129.00
43	GO:0045597	positive regulation of cell differentiation	9.1E-3	10.41	92.00
45	GO:0051241	process	43.0E-3	9.71	104.00
46	GO:0051239	regulation of multicellular organismal process	180.0E-9	9.35	258.00
47	GO:0022008	neurogenesis	40.0E-3	9.12	138.00
48	GO:0032101	regulation of response to external stimulus	5.2E-3	10.88	83.00
49	GO:0050793	regulation of developmental process	3.5E-6	9.41	222.00
50	GO:0030154	cell differentiation	10.0E-9	8.98	339.00
51	GO:0048731	system development	2.3E-12	9.08	405.00
52	GO:0048869	cellular developmental process	780.0E-12	9.03	358.00
53	GO:0048468	cell development	6.8E-3	8.94	177.00
54	GO:0051128	regulation of cellular component organization	17.0E-3	8.57	206.00
55	GO:0050793	regulation of developmental process	3.5E-6	9.41	222.00
57	GO:0051240	positive regulation of multicellular organismal process	5.8E-6	10.28	155.00
57	GO:0048513	animal organ development	43.0E-6	8.68	284.00
58	GO:0009888	tissue development	5.0E-6	9.85	182.00
59	GO:0009653	anatomical structure morphogenesis	100.0E-9	9.57	241.00
59	GO:0007399	nervous system development	700.0E-6	8.98	205.00

NODE	GOID	GO Term	P-Value	% Genes	Nr. Genes
60	GO:0009790	embryo development	26.0E-3	9.89	100.00
61	GO:0072359	circulatory system development	29.0E-6	11.07	111.00
62	GO:0048646	morphogenesis	500.0E-9	11.55	119.00
63	GO:0072358	cardiovascular system development	320.0E-6	11.89	78.00
64	GO:0048514	blood vessel morphogenesis	13.0E-3	11.55	62.00
65	GO:0001944	vasculature development	160.0E-6	12.06	78.00
66	GO:0001568	blood vessel development	250.0E-6	12.04	75.00
67	GO:0043542	endothelial cell migration	9.1E-3	16.37	28.00
68	GO:0010631	epithelial cell migration	980.0E-6	15.51	38.00
69	GO:0001667	ameboidal-type cell migration	3.4E-3	13.35	47.00
70	GO:0090132	epithelium migration	1.2E-3	15.32	38.00
71	GO:0090130	tissue migration	830.0E-6	15.35	39.00
72	GO:0040017	positive regulation of locomotion	2.5E-3	12.45	58.00
73	GO:0030335	positive regulation of cell migration	1.0E-3	13.10	55.00
74	GO:2000147	positive regulation of cell motility	2.8E-3	12.67	55.00
75	GO:0016477	cell migration	4.5E-12	12.17	157.00
76	GO:0048870	cell motility	280.0E-12	11.49	163.00
77	GO:0040012	regulation of locomotion	1.7E-3	10.83	91.00
78	GO:2000145	regulation of cell motility	1.3E-3	11.11	86.00
79	GO:0051272	positive regulation of cellular component movement	1.3E-3	12.81	57.00
80	GO:0051270	regulation of cellular component movement	270.0E-6	11.14	94.00
81	GO:0030334	regulation of cell migration	220.0E-6	11.63	84.00
82	GO:0006928	movement of cell or subcellular component	96.0E-12	10.79	203.00
83	GO:0050900	leukocyte migration	820.0E-6	13.38	53.00
84	GO:0032879	regulation of localization	52.0E-6	9.02	233.00
85	GO:0006935	chemotaxis	1.2E-3	11.86	70.00
86	GO:0042330	taxis	740.0E-6	12.01	71.00
87	GO:0071621	granulocyte chemotaxis	16.0E-3	18.75	21.00
88	GO:0097530	granulocyte migration	25.0E-3	17.74	22.00
89	GO:0097529	myeloid leukocyte migration	6.1E-3	16.38	29.00
90	GO:0051049	regulation of transport	32.0E-3	8.83	166.00
91	GO:0046903	secretion	2.9E-3	10.00	117.00
92	GO:0032940	secretion by cell	630.0E-6	10.50	108.00
93	GO:0007167	enzyme linked receptor protein signaling pathway	1.7E-3	10.34	106.00
94	GO:0007166	cell surface receptor signaling pathway	2.6E-6	9.11	258.00
95	GO:0010564	regulation of cell cycle process	5.6E-3	11.46	69.00
96	GO:0048518	positive regulation of biological process	70.0E-9	8.31	455.00
97	GO:0048522	positive regulation of cellular process	10.0E-9	8.56	418.00
98	GO:0007165	signal transduction	19.0E-6	7.94	478.00
99	GO:0048584	positive regulation of response to stimulus	1.1E-6	9.67	210.00
100	GO:0048583	regulation of response to stimulus	1.6E-9	9.05	347.00
101	GO:0023056	positive regulation of signaling	290.0E-6	9.62	159.00
102	GO:0009967	positive regulation of signal transduction	500.0E-6	9.75	147.00
103	GO:1902533	positive regulation of intracellular signal transduction	28.0E-3	10.00	96.00
104	GO:0042327	positive regulation of phosphorylation	26.0E-3	9.99	98.00
105	GO:0050730	regulation of peptidyl-tyrosine phosphorylation	41.0E-3	14.10	33.00
106	GO:0050731	positive regulation of tyrosine phosphorylation	8.6E-3	16.11	29.00
107	GO:0043408	regulation of MAPK cascade	18.0E-3	10.71	77.00
108	GO:0001934	phosphorylation	17.0E-3	10.12	95.00
109	GO:0071900	kinase activity	20.0E-3	11.72	58.00
110	GO:0023014	phosphorylation	15.0E-3	10.10	97.00
111	GO:0000165	MAPK cascade	27.0E-3	10.06	93.00
112	GO:0016310	phosphorylation	190.0E-6	9.06	214.00
113	GO:0051338	regulation of transferase activity	41.0E-3	9.84	98.00
114	GO:0006793	phosphorus metabolic process	41.0E-3	8.11	266.00
115	GO:0031401	process	41.0E-3	9.49	114.00
117	GO:0036211	protein modification process	21.0E-3	7.98	315.00

NODE	GOID	GO Term	P-Value	%Genes	Nr. Genes
118	GO:0042325	regulation of phosphorylation	47.0E-6	10.11	147.00
119	GO:0006796	process	48.0E-3	8.10	265.00
120	GO:0006464	cellular protein modification process	21.0E-3	7.98	315.00
121	GO:0051174	regulation of phosphorus metabolic process	410.0E-6	9.54	162.00
122	GO:0050790	regulation of catalytic activity	49.0E-3	8.42	208.00
124	GO:0023057	negative regulation of signaling	22.0E-3	9.50	120.00
125	GO:0035556	intracellular signal transduction	120.0E-12	9.81	274.00
126	GO:0010648	negative regulation of cell communication	21.0E-3	9.53	120.00
127	GO:0048585	negative regulation of response to stimulus	2.4E-3	9.59	139.00
129	GO:0048523	negative regulation of cellular process	51.0E-9	8.63	384.00
130	GO:0070887	cellular response to chemical stimulus	180.0E-6	8.79	246.00
131	GO:0009966	regulation of signal transduction	360.0E-9	9.24	265.00
132	GO:0007154	cell communication	1.2E-6	7.96	518.00
133	GO:1902531	transduction	57.0E-6	9.65	175.00
134	GO:0070887	cellular response to chemical stimulus	180.0E-6	8.79	246.00
135	GO:0010033	response to organic substance	6.5E-6	8.97	265.00
136	GO:0071310	cellular response to organic substance	100.0E-6	9.15	211.00
137	GO:0033993	response to lipid	12.0E-3	10.21	96.00
138	GO:0048519	negative regulation of biological process	5.8E-9	8.62	413.00
139	GO:0019220	regulation of phosphate metabolic process	710.0E-6	9.49	161.00
140	GO:0031399	regulation of protein modification process	6.0E-3	9.16	159.00
141	GO:0001932	regulation of protein phosphorylation	170.0E-6	10.08	137.00
142	GO:0045859	regulation of protein kinase activity	15.0E-3	10.62	81.00
143	GO:0043549	regulation of kinase activity	17.0E-3	10.44	86.00
144	GO:0010647	positive regulation of cell communication	110.0E-6	9.74	160.00
145	GO:0008285	negative regulation of cell proliferation	680.0E-6	11.56	80.00

Supplemental Table 2. Verfaillie Invasive Program

Gene	Log2 value	Gene	Log2 value	Gene	Log2 value	Gene	Log2 value
ADAM19	-2.3	FOSL1	1.52	NUAK2	1.392	TGM2	1.306
ADAMTS6	1.793	FSTL3	1.519	OASL	1.392	THBS1	1.306
ALPK2	1.775	GLIPR1	1.517	OSMR	1.389	THSD4	1.306
AMPD3	1.775	GNAI2	1.517	OXTR	1.388	TMEM158	1.305
ANGPTL4	1.772	GRAMD1B	1.515	PCDH10	1.388	TNFAIP2	1.305
ARHGAP22	1.772	HBEGF	1.514	PDGFB	1.386	UBE2E3	1.303
ARL4C	1.767	HMGA1	1.513	PDLIM5	1.385	VEGFA	1.303
ASPH	1.76	HRH1	1.51	PDLIM7	1.384	VEGFC	1.302
ATP2B1	1.749	HSPA5	1.509	PLAUR	1.383	WNT5A	1.299
AXL	1.736	HSPB7	1.5	PLK2	1.383	ZNF185	1.298
BCL3	1.735	HTR7	1.499	PLOD2	1.383		
BDNF	1.731	ID1	1.498	POU2F2	1.381		
BIRC3	1.73	IFI44L	1.488	PVR	1.381		
CA9	1.729	IGFBP3	1.485	RASA3	1.378		
CCL5	1.725	IGFBP6	1.484	RELB	1.377		
CD274	1.721	IGFN1	1.484	RGS4	1.374		
CD96	1.714	IL11	1.476	RIN1	1.373		
CDH6	1.713	IL1B	1.471	RND3	1.371		
CLEC2B	1.703	IL4I1	1.466	RRAS2	1.371		
CNN2	1.696	IL6	1.46	S100A16	1.368		
COL13A1	1.695	IL6ST	1.458	S100A4	1.367		
COL1A1	1.669	IL7R	1.457	SCG2	1.362		
COL1A2	1.665	IL8	1.457	SCN2A	1.359		
CPA4	1.642	INHBA	1.455	SEC24D	1.358		
CPE	1.64	IRS1	1.449	SEMA4B	1.356		
CREB3L1	1.618	ITGA2	1.447	SERPINB2	1.354		
CSF1	1.617	ITGA5	1.447	SERPINB7	1.354		
CXCL1	1.616	ITGB1	1.446	SERPINE1	1.345		
CXCL3	1.601	JUN	1.443	SH3RF2	1.344		
CYP27C1	1.6	KANK2	1.443	SIAH2	1.341		
DCN	1.599	KCTD1	1.443	SKIL	1.338		
DDAH1	1.593	KLF7	1.44	SLC10A3	1.336		
DENND2A	1.592	KRT18	1.44	SLIT2	1.336		
DKK1	1.589	KRT8	1.436	SNED1	1.335		
DOCK2	1.589	KRT80	1.435	SOX9	1.335		
EDIL3	1.582	LAMA3	1.43	SPEG	1.335		
EFEMP2	1.582	LAMB3	1.427	SPOCD1	1.332		
EFHD2	1.579	LASP1	1.426	SPOCK1	1.331		
EFNB2	1.578	LOXL2	1.423	SPRED3	1.331		
ELL2	1.578	LTBP1	1.42	SRGN	1.326		
EPS8L2	1.576	LTBP2	1.419	SRPX2	-2.359		
EXT1	1.568	MAP4K4	1.418	ST6GALNAC4	-2.368		
FAM129B	1.563	MPP4	1.417	STC1	-2.368		
FAM196B	1.563	MT2A	1.417	STEAP2	-2.368		
FAM20C	1.561	MYPN	1.415	STX1A	-2.375		
FAM84A	1.555	NCEH1	1.411	SYDE1	-2.379		
FBN1	1.548	NNMT	1.408	SYT1	-2.394		
FEZ2	1.548	NPTX1	1.407	TAGLN	-2.395		
FGF5	1.547	NR2F1	1.405	TBX3	-2.402		
FJX1	1.536	NRP1	1.398	TFPI	-2.414		
FLNB	1.521	NTNG1	1.395	TGFBR2	1.307		

Supplemental Table 3. Verfaillie Proliferative Program

Gene	Log2 value	Gene	Log2 value	Gene	Log2 value	Gene	Log2 value	Gene	Log2value
ABCB5	-2.741	EIF4EBP2	0.849	MAD2L1BP	-0.811	PSEN2	-0.735	USP6N	0.819
ACO2	1.201	EN2	-0.865	MAF	1.932	RAB17	-1.321	VAT1	0.598
ACSL1	-0.925	ENTHD1	-1.783	MAP3K1	-0.788	RAB3A	-1.034	VGF	-3.011
ADAM10	1.395	ERBB3	0.718	MAP6D1	-0.724	RASEF	-0.987	WDFY1	1.053
ADCY2	-1.200	FAM101B	-0.635	MAPK4	-1.326	REEP6	-1.015	WIPF3	-0.928
AGPAT6	0.644	FAM134B	-2.127	MAST1	-0.605	RGS1	-2.628	WIPI1	-0.777
ALDH3B2	-0.851	FAM149A	1.416	MBP	0.897	RHBDD3	0.580	ZNF704	0.653
AMDHD2	0.945	FAM189A2	0.704	MERTK	-1.969	RHPN1	-1.097		
ANKRD44	0.912	FAM53B	1.098	MFAP3L	-0.808	SAMD5	-1.027		
APOE	0.937	FAM69C	1.118	MGAT4A	-0.909	SASH1	0.840		
ARHGAP1	-1.294	FARP1	0.783	MLIP	0.745	SBK1	0.996		
ARNT2	-1.362	FARP2	-0.610	MMP8	-1.891	SCD	-1.500		
ARSG	-0.939	FASN	-0.721	MOAP1	-1.261	SEC11C	-0.601		
ASB4	-0.600	FCRLA	-1.626	MPPED2	1.331	SEMA6D	1.095		
ASRGL1	0.581	FRMD3	-0.588	MPZ	1.509	SESN3	1.148		
AVP1	-0.978	GALNT3	0.680	MSI2	0.654	SH3TC1	-0.975		
BCAN	2.068	GDPD5	1.108	MYH10	0.734	SIRPA	0.640		
BCL2	0.842	GJB1	-2.483	MYLIP	0.900	SLAIN1	-1.214		
BIN3	-0.635	GK	-0.835	MYO10	0.620	SLC16A6	1.923		
BIRC7	-2.678	GLUD2	-1.583	NAT8L	-0.714	SLC22A23	-1.020		
C11orf96	-2.728	GOLGA7B	-1.327	NEDD9	0.591	SLC23A2	-0.782		
C1orf85	0.645	GPM6B	0.7315	NKAIN1	-1.742	SLC25A16	1.455		
CABLES1	1.209	GPR153	0.896	NR4A1	-2.199	SLC35F1	-1.376		
CACNA1H	-1.636	GPR19	1.306	NR4A3	-1.890	SLC39A11	-0.875		
CDH19	-1.061	GREB1	0.9382	NUP210	-0.599	SLC7A4	-1.224		
CDH3	-1.126	HEY1	-0.8471	OSTM1	-0.903	SOX13	-0.836		
CDC42	1.256	HSD17B14	1.384	PAEP	-4.313	SSH2	0.583		
CDKN1A	1.167	HSF4	0.7608	PARD6G	0.685	ST6GAL1	-1.283		
CDKN2B	-1.569	IGF1	1.405	PAX3	0.652	STX3	-1.077		
CDKN1B	0.652	IGSF8	-1.184	PDGFD	-3.016	STXBP1	-1.453		
CDKN2C	2.055	IL16	0.601	PDK4	-1.343	TAB3	0.717		
CHST11	-1.045	IL6R	-1.074	PDZRN3	1.038	TBC1D14	0.619		
CHST6	-1.000	INPP5F	-0.7274	PFKFB2	-0.889	TBC1D16	0.745		
CLCN7	0.756	IRF4	1.126	PHACTR1	0.595	TCFL5	0.795		
COL9A3	0.681	IRX6	0.9298	PKNOX2	0.904	TCTN3	-1.101		
CPN1	-0.653	ISG20	-2.45	PLCL1	4.489	TESK2	-0.685		
CPVL	-1.750	ITGA7	-2.521	PLEKHG3	0.871	TFAP2A	0.859		
CRYL1	0.932	ITGAX	-3.94	PLP1	0.736	TKTL1	-1.384		
CTSH	1.218	KBTBD11	-1.072	PLXNC1	0.798	TLE1	1.228		
CXADR	-1.849	KCP	-1.834	PNLI PRP3	-1.735	TMC6	-0.744		
CYP27A1	0.869	KIAA1211	0.9392	PNMAL1	-1.267	TMEM170	-0.812		
DAAM1	0.588	KI67	1.1340	POLR3G	-0.936	TMEM229	1.244		
DENND1C	-1.710	KLF15	-0.6169	POU3F2	-0.604	TMEM33	-1.342		
DHTKD1	-0.787	LCP2	-3.637	PPFIBP2	1.510	TMEM64	-0.721		
DLL3	0.632	LDLRAD3	0.6759	PPFIBP3	1.675	TOP2A	1.376		
DUSP22	0.955	LGI3	-0.6352	PPP1R14C	-1.140	TP53	1.293		
EFR3B	-0.610	LONRF3	-2.127	PPP1R3D	-0.786	TPCN2	1.286		
EGLN3	0.993	LRP2	-0.7623	PRKD3	0.677	TPD52	-1.621		
EGR3	-5.208	LZTS1	0.8597	PRODH	3.501	TRIB2	-0.973		
EIF4EBP2	0.850	MAD2L1B	-0.8111	PRSS33	-1.873	TRPM8	-2.114		
EN2	-0.866	MAF	1.932	PRUNE2	-1.483	TSPAN3	-0.652		

Supplemental Table 4. Overlapping genes with MITF and AXL Program

Low vs High SMAD7(TCGA)				siSMAD7 vs siCtrl			
MITF Program		AXL Program		MITF Program		AXL Program	
MLANA	3.361	UCN2	-3.425	PLK2	1.739	UBE2C	0.876
RAB38	3.208	SLC16A6	-3.194	JUN	1.300	GADD45A	0.783
ABCB5	3.008	TCN1	-2.173	CELF2	1.160	FSTL3	0.582
HMCN1	3.361	CITED1	-2.116	IRF4	1.120	UPP1	1.854
CDK2	3.252	ENO2	-2.054	APOE	0.937	FN1	1.250
SLC7A5	2.821	UPP1	-1.794	ELOVL2	0.860	GLRX2	0.654
VAT1	2.818	PFKFB4	-1.671	CYP27A1	0.856	UBE2J1	0.709
PTPRZ1	2.786	ANGPTL4	1.043	LZTS1	0.856	RIN1	-0.709
MLPH	2.458	GLRX	1.103	TFAP2A	0.855	SLC16A3	0.731
TFAP2A	2.56	GEM	1.168	PLP1	0.736	ZYX	0.774
TYR	2.36	IL18BP	1.251	ERBB3	0.718	P4HA2	0.775
CDH1	2.346	SPATA13	1.277	C1orf85	0.645	GBE1	0.818
TMEM98	1.987	FAM46A	1.292	SIRPA	0.640	NGFR	0.820
GYG2	1.954	COL6A1	1.302	MYO10	0.620	C9orf89	0.821
SLC24A5	1.877	LOXL2	1.352	VAT1	0.598	SH3BGR3	0.832
MITF	1.65	ZCCHC6	1.374	STAM	0.589	SLC25A37	0.871
PIR	1.876	FGFRL1	1.391	SLC35B4	-0.743	FOSL1	0.887
SNCA	1.765	FN1	1.478	OSTM1	-0.903	TIMP1	0.892
C1orf85	1.721	HAPLN3	1.492	IGSF8	-1.184	HPCAL1	0.900
IGSF8	1.718	COL6A2	1.531	DNAJA4	-1.938	FAM46A	0.923
GPR143	1.717	BACH1	1.555	FOSB	-3.104	DBNDD2	0.933
DNAJA4	1.678	CADM1	1.598			PHLDA2	0.953
IGSF11	1.567	CRIP1	1.62			FGFRL1	1.026
CHL1	1.423	SLC22A4	1.665			LOXL2	1.034
QPCT	1.346	NNMT	1.717			TNFRSF12	1.073
TBC1D7	1.325	S100A4	1.785			CD82	1.107
JUN	1.45	AIM2	1.821			SEC14L2	1.134
SIRPA	1.235	PMAIP1	1.836			S100A6	1.141
CYP27A1	1.235	IGFBP3	1.876			CDKN1A	1.167
TNFRSF1	1.234	MAP1B	1.942			SERPINE1	1.191
SLC45A2	1.16	CD52	2.071			MT2A	1.335
EXOSC4	1.168	SERPINE1	2.124			SLC2A1	1.338
CAPN3	1.982	CHI3L1	2.139			ENO2	1.358
LZTS1	1.152	AXL	2.242			CD109	1.368
S100B	1.126	NGFR	2.259			ERO1L	1.142
SLC19A2	1.123	CFB	2.456			AIM2	1.358
ROPN1	0.765	STRA6	2.982			AXL	1.498
FOSB	1.565					MAP1B	1.500
DOCK10	1.855					PLAUR	1.796
ELOVL2	2.346					NNMT	1.830
						IL8	1.358
						IGFBP3	1.358
						GEM	3.632
						UCN2	4.248
						METTL7B	5.479
						ANGPTL	1.358

Supplemental Table 5. FACS for EdU/MITF/AXL staining under different treatments

Sample Treatment		Statistics	#Cells (200000)	Average
siCtrl	EdU AXL ^{high} MITF ^{low}	3.19	684	3.53
siCtrl	EdU AXL ^{high} MITF ^{low}	3.48	696	
siCtrl	EdU AXL ^{high} MITF ^{low}	3.69	738	
siSmad7	EdU AXL ^{high} MITF ^{low}	2.38	476	3.17
siSmad7	EdU AXL ^{high} MITF ^{low}	3.59	618	
siSmad7	EdU AXL ^{high} MITF ^{low}	3.54	708	
siCtrl	EdU AXL ^{low} MITF ^{high}	22.39	4378	20.26
siCtrl	EdU AXL ^{low} MITF ^{high}	18.78	3756	
siCtrl	EdU AXL ^{low} MITF ^{high}	20.12	4024	
siSmad7	EdU AXL ^{low} MITF ^{high}	18.72	3740	19.43
siSmad7	EdU AXL ^{low} MITF ^{high}	19.11	3820	
siSmad7	EdU AXL ^{low} MITF ^{high}	20.52	4100	
siCtrl	EdU AXL ^{high} MITF ^{high}	2.01	402	1.81
siCtrl	EdU AXL ^{high} MITF ^{high}	1.98	396	
siCtrl	EdU AXL ^{high} MITF ^{high}	1.20	290	
siSmad7	EdU AXL ^{high} MITF ^{high}	1.95	380	2.08
siSmad7	EdU AXL ^{high} MITF ^{high}	2.07	474	
siSmad7	EdU AXL ^{high} MITF ^{high}	2.21	542	

Sample Treatment		Statistics	#Cells (200000)	Average
siCtrl + TGFB2+ BMP7	EdU AXL ^{high} MITF ^{high}	6.39	1278	6.13
siCtrl TGFB2+ BMP7	EdU AXL ^{high} MITF ^{high}	5.74	1096	
siCtrl TGFB2+ BMP7	EdU AXL ^{high} MITF ^{high}	6.51	1302	
siSMAD7 TGFB BMP7	EdU AXL ^{high} MITF ^{high}	9.56	1912	10.06
siSMAD7 TGFB BMP7	EdU AXL ^{high} MITF ^{high}	11.48	2296	
siSMAD7 TGFB BMP7	EdU AXL ^{high} MITF ^{high}	9.14	1828	
siCtrl + TGFB BMP7	EdU AXL ^{low} MITF ^{high}	26.71	5342	25.28

siCtrl +TGFB BMP7	EdU AXL ^{low} MITF ^{high}	28.95	5730	22.77
siCtrl +TGFB BMP7	EdU AXL ^{low} MITF ^{high}	20.47	4094	
siSMAD7+TGFB BMP7	EdU AXL ^{low} MITF ^{high}	25.89	5178	
siSMAD7+TGFB BMP7	EdU AXL ^{low} MITF ^{high}	20.12	4024	
siSMAD7+TGFB BMP7	EdU AXL ^{low} MITF ^{high}	22.31	4462	
siCtrl TGFB + BMP7	EdU AXL ^{high} MITF ^{low}	4.31	862	3.85
siCtrl TGFB + BMP7	EdU AXL ^{high} MITF ^{low}	3.25	650	
siCtrl TGFB + BMP7	EdU AXL ^{high} MITF ^{low}	3.98	796	
siSMAD7+ TGFB2 + BMP7	EdU AXL ^{high} MITF ^{low}	10.70	2298	12.85
siSMAD7+ TGFB2 + BMP7	EdU AXL ^{high} MITF ^{low}	9.65	1854	
siSMAD7+ TGFB2 + BMP7	EdU AXL ^{high} MITF ^{low}	13.25	2201	

Supplemental Table 6. MFI levels for MITF

Samples	Q1EdU ⁺ AXL ⁻	Q2EdU ⁺ AXL ⁺	Q3EdU ⁻ AXL ⁻	Q4EdU ⁻ AXL ⁺
No treatment	2548	1189	1547	1105
No treatment	2200	1140	1496	154
No treatment	2148	1257	1440	1298
siCtrl	2479	1205	1385	1145
siCtrl	2319	1225	1350	1039
siCtrl	2079	1154	1278	1223
siSmad7	2371	1098	1584	1354
siSmad7	2230	1146	1503	1159
siSmad7	2183	1668	1445	1198
siCtrl+ TGF-β2+BMP7	2854	1539	1496	1014
siCtrl+ TGF-β2+BMP7	2793	1679	1357	1204
siCtrl+ TGF-β2+BMP7	2935	1300	1547	1158
siSmad7+TGF-β2+BMP7	2194	2553	1143	1053
siSmad7+TGF-β2+BMP7	2031	2403	1443	1125
siSmad7+ TGF-β2+BMP7	2217	2247	1284	1185

Supplemental Table 7. Mouse Genotyping Primers

Gene	Forward Sequence (5'-3')	Reverse Sequence (5'-3')
<i>Cre</i>	CTATCCAGCAACATTTGGGCCAGC	CCAGGTTACGGATATAGTTCATGAC
<i>Ink4^{wt}</i>	ATGATGATGGGCAACGTTCC	CAAATATCGCACGATGTC
<i>Ink4^{-/-}</i>	CTATCAGGACATAGCGTTGG	AGTGAGAGTTTGGGGACAGAG
<i>N-Ras^{Q61K}</i>	GATCCCACCATAGAGGATT	CTGGCGTATTTCTCTTACC
<i>Smad4^{wt}</i>	GGCACATTACATTTGCAGTCAG	AGGAAAAACAGGGCTATGTAGAA
<i>Smad4^{lox}</i>	GGCACATTACATTTGCAGTCAG	GACCCAAACGTCACCTTCAC
<i>Smad7^{wt}</i>	TTCAGAGGCAGACCGAACCTCCAA	AGGATTGGGTCAGGGACAGAAGAGCA
<i>Smad7^{lox}</i>	TTCAGAGGCAGACCGAACCTCCAA	TCTCACCTTGCTCCTGCCGAGAAAGTA
<i>LacZ</i>	GGTCGGCTTACGGCGGTGATTT	AGCGGCGTCAGCAGTTGTTTTT

Supplemental Table 8. Antibodies

Primary Antibodies				
Antigen	Company/Location	Source	Application / Dilutions	Catalog/Clone Number
β -actin	Sigma- Aldrich, Missouri, USA	Mouse	WB 1:10000	A-5316 / AC-74
α -tubulin	Sigma- Aldrich, Missouri, USA	Mouse	WB 1:10000	T-6074 / D
β -Gal.	Abcam, Cambridge, UK	Chicken	IF 1:1000	ab9361/polyclonal
Axl	Santa Cruz, Texas, USA	Goat	WB 1:50 IF 1:100	sc-1096 / C-20
AXL	Cell Signaling Technology, USA	Rabbit	FACS 1:1000	C89E7/8661
Caspase3	Cell Signaling Technology, USA	Rabbit	IF 1:200	9661/polyclonal
DCT	Santa Cruz Biotechnology, USA	Goat	IF 1:250	sc-10451/polyconal
Anti-Melanoma	Abcam Cambridge, UK	Mouse	IF 1:200	ab732/HMB45,M2-7C10,M2-9E3
pSMAD2/3	Santa Cruz, Texas, USA	Goat	IF 1:300	sc-11769/polyclonal
pSMAD2	Cell Signaling Technology, USA	Rabbit	WB 1:50 IF 1:300	3101/polyclonal
pSMAD1/5/8	Cell Signaling Technology, USA	Rabbit	WB 1:50 IF 1:300	9511S/41D10
SMAD2	Cell Signaling Technology, USA	Rabbit	WB 1:100	5339/D43B4
SMAD1	Cell Signaling Technology, USA	Rabbit	WB 1:50	9743
PAX3	Invitrogen, California, USA	Rabbit	IF 1:300	38081/polyclonal
SMAD7	Santa Cruz, Texas, USA	Goat	IF 1:300	sc-365846/B-8
SMAD7	RD System, Minnesota, USA	Mouse	IF1:100	/293039MAB2029
SMAD4	Abcam Cambridge, UK	Rabbit	IF 1:300	ab40759/EP618Y
Ki67	Abcam Cambridge, UK	Rabbit	IF 1:50	ab15580/polyclonal
MITF	Santa Cruz, Texas, USA	Rabbit	IF, FACS1:500	sc-56726/D-5
Zeb1	Bethyl Laboratories, Texas, USA	Mouse	IF1:300	IHC-00419/polyclonal

ZEB1	Santa Cruz, Texas, USA	Rabbit	IF1:200	H102/polyclonal
MITF	Heinz Arnheiter, NIH,USA	Mouse	IF1:500 FACS1:1000	clone 6D3,
Cdkn2a(p16)	Santa Cruz, Texas, USA	Mouse	WB1:200	sc-1661/F-12
Cdkn1a(p21)	Santa Cruz, Texas, USA	Rabbit	WB1:200	sc-1064/polyclonal
Cdkn1b(p27)	Cell Signaling Technology, USA	Mouse	WB1:200	2552/polyclonal
Cdkn1c(p57)	Cell Signaling Technology, USA	Rabbit	WB1:200	2557/polyclonal
Cdkn2c(p18)	Cell Signaling Technology, USA	Rabbit	WB1:200	DCS118/2896

Secondary Antibodies				
Antigen	Company	Source	Application	Catalog Number
Alexa 546	Jackson ImmunoResearch, Cambridgeshire, UK	Mouse	IF,FACS:1:250	Cat#A-1103/IgG H+L
Alexa 488	Jackson ImmunoResearch, Cambridgeshire, UK	Rabbit	IF1:250	Cat#711-545-152/IgG H+L
Alexa 488	Jackson ImmunoResearch, Cambridgeshire, UK	Goat	IF,FACS:1:250	Cat#705-545-147/IgG H+L
Alexa-647	Jackson ImmunoResearch, Cambridgeshire, UK	Donkey	IF 1:250	Cat#715-605-150/IgG H+L
Biotin-SP IgG	Jackson ImmunoResearch, Cambridgeshire, UK	Donkey	IF 1:300	Cat#711-065-052
Biotin-SP IgG	Chemicon, Osaki, Japan	Chicken	IF 1:300	Cat#AP194B/IgGL
Streptavidin HRP	Jackson ImmunoResearch, Cambridgeshire, UK	Goat	IF 1:300	Cat#016-030-084/IgG H
IRDye-800CW	Li-COR Biosciences, Lincoln, USA	Donkey	WB 1:10000	Cat#926-32214/IgG H+L
IRDye-680LT	Li-COR Biosciences, Lincoln, USA	Mouse	WB 1:10000	Cat#926-68023/IgG H+L

Supplemental Table 9. siRNAs and Primer sequences

Forward and reverse primer sequences used in qPCR and the sequences of the siRNAs aimed against the different SMADs

Human(siRNA)

Gene	Company	Target Exon	siRNA Location	Catalog Number
siSMAD7 #1	Life Technologies, California, USA	Human 3,4	1028	Cat#HSS106264
siSMAD7 #2	Life Technologies, California, USA	Human 4	1426	Cat#HSS180976
siSMAD4 #1	Life Technologies, California, USA Life Technologies	Human 9,10	1582	Cat#HSS106255
siSMAD4 #2	Life Technologies, California, USA Life Technologies	Human 4	1088	Cat#HSS180972
siControl Med.GC	Life Technologies, California, USA Life Technologies	Human		Cat#129353003

Human (RT-PCR Primers)

Primers provided by Microsynth, Balgach, Switzerland		
Genes	Forward Sequence (5'-3')	Reverse Sequence (5'-3')
ACTIN	AGAGCTACGAGCTGCCTGAC	AGCACTGTGTTGGCGTACAG
AXL	GCTGTCAGACGATGGGATG	CCATTCCGCGTAGCACTAA
GAPDH	AATCCCATCACATCTTCC	CATCACGCCACAGTTTCC
ZEB1	TGCACTGAGTGTGGAAAAGC	TGGTGATGCTGAAAGAGACG
TWIST1	ACCATCCTCACACCTCTGCATT	TGCAGGCCAGTTTGTATCCAGTAT
ZEB2	CGCTTGACATCACTGAAGGA	CTTGCCACACTCTGTGCATT
SNAIL2	AGCAAGAAGTCGAGCGAAGA	CAGCTTGAGCGTCTGGATCT
CDH1	CTGCTGCCACCAGATGATGA	CTGTGCAGCTGGCTCAAATC
CDH271	CCT ACGGCTACTACCAGGATG	CACACGGTGTCTGCTTGT
MITF	CAGGCATGAACACACATTCAC	TCCATCAAGCCCAAGATTTTCC
VIM	GAGAACTTTGCCGTTGAAGC	GCTTCCTGTAGGTGGCAATC
FN1	AAACCAATTCTTGGAGCAGG	CCATAAAGGGCAACCAAGAG
AXL	GCTGTCAGACGATGGGATG	CCATTCCGCGTAGCACTAAT
CDK2	TTCTGCCATTCTCATCGGGT	AGGAGGATTTTCCAGGAGCTCG
CDKN1A	GACCATGTGGACCTGTCACT	GGAGTGGTAGAAATCTGTCAATG
CDKN1B	TAATTGGGGCTCCGGCTAAC	AGAAGAATCGTCGGTTGCAG
CDKN1C	CAAGAGATCAGCGCCTGAGA	CTCTTTGGGCTTTGGCTCAC
CDKN2A	AGGTCCCTCAGAAATGATCGG	CAGCCAGCTTGCATAACCA
CDKN2B	GGATCCCAACGGAGTCAACC	CCAACGGAGACTCCTGTACAAA
CDKN2C	CGACTAATTCATCTTTTCTGATCG	GGGATTTCCAAGTTTCATAACCTGC

Human (RT-PCR Primers)

Primers provided by Microsynth, Balgach, Switzerland		
Genes	Forward Sequence (5'-3')	Reverse Sequence (5'-3')
TYRP1	CCGAAACACAGTGGAAGGTT	TCTGTGAAGGTGTGCAGGA
DCT	AGC AGTATGGCTGGAGCA CT	AGCAGTATGGCTGGAGCACT
PMEL	AATCCCATCACATCTTCC	CATCACGCCACAGTTTCC
MC1A	TGCACTGAGTGTGAAAAGC	TGGTGATGCTGAAAGAGACG
MITF	ATGCTGAAAATGCTAGAATACA	CTAACACGCATGCTCCGTTT
SILV	CGCTTGACATCGATAAGGA	ACTTGCCACACTCTGTGCATT
OCA	AGCAAGAAGTCGAGCGAAGA	CAGCTTGAGCGTCTGGATCT

Mouse (RT-PCR Primers)

Genes	Forward Sequence (5'-3')	Reverse Sequence (5'-3')
Actin	GACGGGGTCACCCACACTGTGCCCATCTA	CTAGAAGCATTTCGGGTGGACGATGGAGG
Gapdh	AATCCCATCACATCTTCC	CATCACGCCACAGTTTCC
Zeb1	TGCACTGAGTGTGAAAAGC	TGGTGATGCTGAAAGAGACG
Twist1	ACCATCCTCACACCTCTGCATT	TGCAGGCCAGTTTGATCCCAGTAT
Zeb2	CGCTTGACATCACTGAAGGA	CTTGCCACACTCTGTGCATT
Snail2	AGCAAGAAGTCGAGCGAAGA	CAGCTTGAGCGTCTGGATCT
Cdh1	CTGCTGCCACCAGATGATGA	CTGTGCAGCTGGCTCAAATC
Cdh271	TGCTGTTGCTGCTTCTGG	CTCACACACGGTCTGGTTG
Vim	GAGAACTTTGCCGTTGAAGC	GCTTCCTGTAGGTGGCAATC
Bmp7	ATTTTCAGCCTGGACAACGAG	AGACGGCCTTGTAGGGGTAG
Nodal	ACTTTGCTTTGGGAAGCTGA	AGGAGGGTCAAGTTCCAGGT
Tgfβ2	TGCCAGTGGTGATCAGAAAA	TCCATTTCCATCCAAGATCC
Fn1	AAACCAATTCTTGGAGCAGG	CCATAAAGGGCAACCAAGAG
Cdkn1a	ACGGTGGAACTTTGACTT CG	CAG GGC AGA GGA AGT ACT GG
Cdkn1b	AGTCAGCGCAAGTGGAAATTT	GGTCCTCAGAGTTTGCCTGA
Cdkn1c	CTGACCTCAGACCCAATTCC	CTAGA GACCGGCTAGT TC
Cdkn2a	CCGCTGCAGACAGACTGG	CCATCATCATCACCTGAATCG
Cdkn2b	TTACCAGACCTGTGCACGAC	GCAGATACCTCGCAATGTCA
Cdkn2c	CTGGAGTTCCAGGCGATGT	CCTCCATCAGGCTAATGACC

Supplemental Table 10. Ligands, Chemicals, Cell lines

Ligands	Company	Source	Application / Dilutions	Catalog Number
TGF-β1	R&D Systems, Minnesota, USA	Human	10 ng/μl	Cat#240-B-010
TGF-β2	PeptoTech, London, UK	Human	5-10 ng/μl	Cat#100-35B
ACTIVIN	R&D Systems, Minnesota, USA	Human	50 ng/μl	Cat#338-AC-010
NODAL	R&D Systems, Minnesota, USA	Human	100 ng/μl	Cat#3218-ND-025

BMP2	PeproTech, London, UK	Human	50 ng/μl	Cat#120-02
BMP4	R&D Systems, Minnesota, USA	Human	50 ng/μl	Cat#314-BP
BMP7	R&D Systems, Minnesota, USA	Human	100 ng/μl	Cat#354-BP

Chemicals	Company	Catalog/ Cas Number
Agarose	AppliChem	Cat# A8963; CAS# 9012-36-6
Antibody Diluent	Dako	Cat# S0809
Bovine Serum Albumin (BSA)	Sigma-Aldrich	Cat# A4503; CAS# 9048-46-8
Crystal violet solution	Sigma-Aldrich	Cat# HT90132; CAS# 548-62-9
Dimethyl sulfoxide (DMSO)	Sigma-Aldrich	Cat# D2650; CAS# 67-68-5
DNase I	Roche	Cat# 10104159001; CAS# 9003-98-9
Ethanol absolut	VWR Chemicals	Cat# 20821.296; CAS# 64-17-5
Falcon Cell Strainers, 40 μm	Thermo Fisher Scientific	Cat# 352340
Fetal Cow Serum (FCS)	Thermo Fisher Scientific	Cat# 16140
Fibronectin	Sigma-Aldrich	Cat# F1141
Fluorescent Mounting Medium	Dako	Cat# S3023
Formaldehyde Solution,37%	Sigma-Aldrich	Cat# F8775; CAS# 50-00-0
Fungizone Antimycotic	Thermo Fisher Scientific	Cat# 15290
Glycine	Sigma-Aldrich	Cat# G8898; CAS# 56-40-6
Glycogen	Sigma-Aldrich	Cat# G0885; CAS# 9005-79-2
L-Glutamine	Thermo Fisher Scientific	Cat# 25030
Halt	Thermo Fisher Scientific	Cat# 78440
HEPES	Sigma-Aldrich	Cat# H4034; CAS# 7365-45-9
Hoechst 33342	Sigma-Aldrich	Cat# 14533; CAS# 23491-52-3
Horseshoe Peroxidase-	Jackson ImmunoResearch	Cat# 016-030-084
4-Hydroxytamoxifen (4-SOHT)	Sigma-Aldrich	Cat# H7904; CAS# 68047-06-3
Isoflurane	Piramal Healthcare	Cat# 430024079
Isopropanol	Merck Millipore	Cat# 1096341000; CAS# 67-63-0
Laemmli Sample Buffer, 4X	Bio-Rad	Cat# 1610747
Liberase, DH Research Grade	Roche	Cat# 05401054001
LightCycler 480 Multiwell Plate	Roche	Cat# 04729692001
Medium, DMEM	Thermo Fisher Scientific	Cat# 41965
Medium, DMEM/F-12	Thermo Fisher Scientific	Cat# 21041
Medium, RPMI 1640	Thermo Fisher Scientific	Cat# 42401
2-Mercaptoethanol	Sigma-Aldrich	Cat# M3148; CAS# 60-24-2
Methanol	Merck Millipore	Cat# 106009; CAS# 67-56-1
4-20% Mini-PROTEAN TGX	Bio-Rad	Cat# 4561094, 4561096
NewBlot Nitro Stripping Buffer,	LI-COR Biosciences	Cat# 928-40030
Nitrocellulose/Filter Paper	Bio-Rad	Cat# 1620215
Nonidet P 40 Substitute	Sigma-Aldrich	Cat# 74385; CAS# 9016-45-9
Nuclease S7	Roche	Cat# 10107921001; CAS# 9013-53-0
Odyssey Blocking Buffer	LI-COR Biosciences	Cat# 927-40000
Penicillin-Streptomycin	Thermo Fisher Scientific	Cat# 15070
Phenol-Chloroform-Isoamyl	Sigma-Aldrich	Cat# P3803
Phosphate Buffered Saline	Thermo Fisher Scientific	Cat# 10010
Polybrene	Santa Cruz Biotechnology	Cat# sc-134220
Potassium chloride	Sigma-Aldrich	Cat# P9333; CAS# 7447-40-7
PRI-724, Canonical WNT	Selleckchem	Cat# S8262; CAS# 847591-62-2
Protein A-Sepharose CL-4B	GE Healthcare	Cat# 17-0780-01
Protein LoBind Tubes	Eppendorf	Cat# 0030108116
Proteinase K, recombinant PCR	Roche	Cat# 03115828001

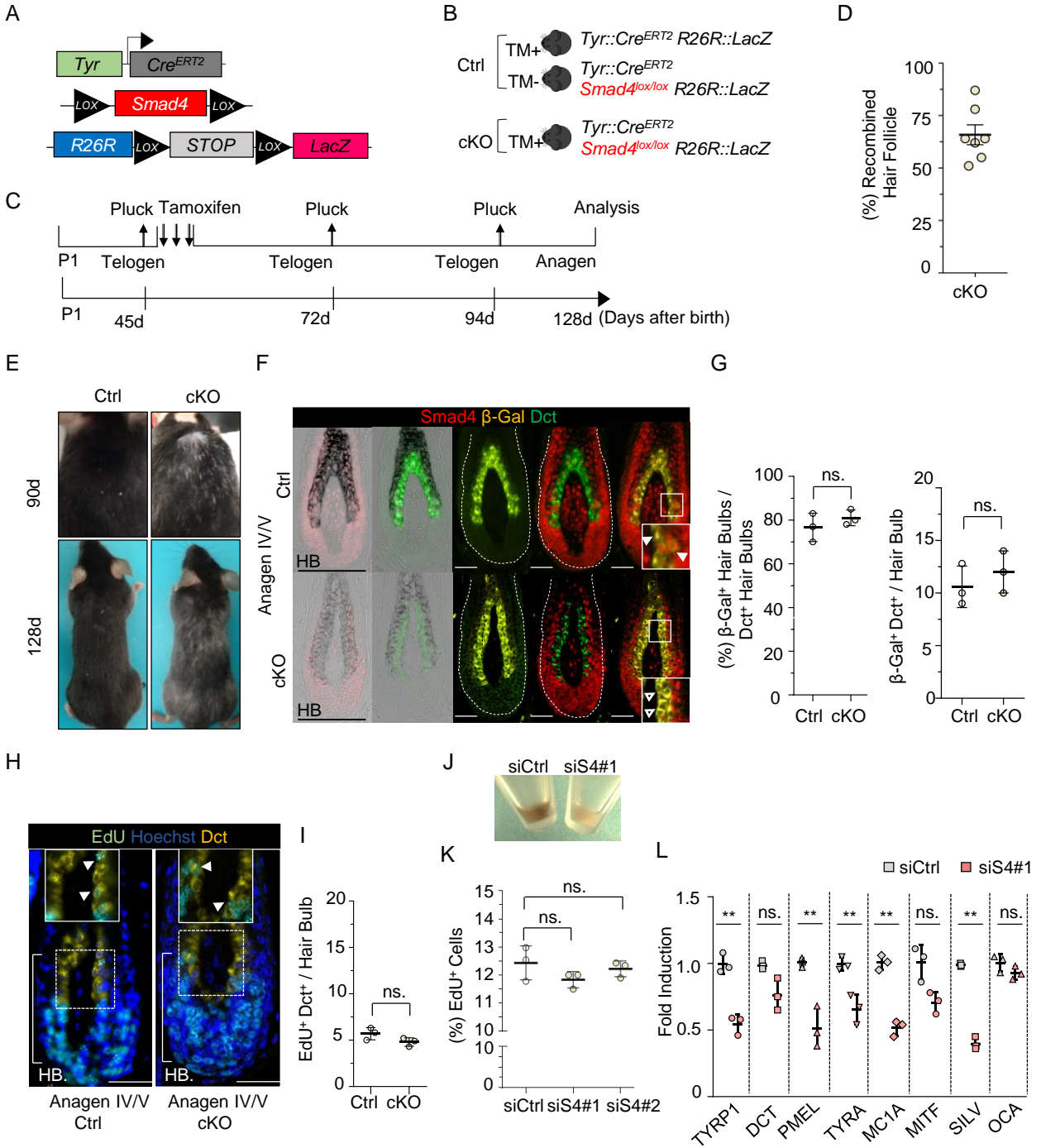
RIPA Buffer	Thermo Fisher Scientific	Cat# 89900
RLT Buffer	Qiagen	Cat# 79216
RNase H	Thermo Fisher Scientific	Cat# EN0202
Roti-Histofix, 4%	Carl Roth	Cat# P087.3
SHH, Recombinant human	PeproTech	Cat# 100-45
Sodium acetate, anhydrous	Sigma-Aldrich	Cat# W302406; CAS# 127-09-3
Sodium chloride	Sigma-Aldrich	Cat# 71380; CAS# 7647-14-5
Sodium deoxycholate	Sigma-Aldrich	Cat# 30970; CAS# 302-95-4
Sodium dodecylsulfate	AppliChem	Cat# A2263; CAS# 151-21-3
Sucrose	Sigma-Aldrich	Cat# S0389; CAS# 57-50-1
Sunflower seed oil	Sigma-Aldrich	Cat# S5007; CAS# 8001-21-6
Tamoxifen (TM)	Sigma-Aldrich	Cat# T5648; CAS# 10540-29-1
Target Retrieval Solution,	Dako	Cat# S2369
Tetradecanoylphorbol 13-	Sigma-Aldrich	Cat# P1585; CAS# 16561-29-8
Tris Hydrochloride	AppliChem	Cat# A3452; CAS# 1185-53-1
Tris/Glycine Buffer, 10X	Bio-Rad	Cat# 1610734
Tris/Glycine/SDS Buffer, 10X	Bio-Rad	Cat# 1610732
Triton X-100	Sigma-Aldrich	Cat# T8787; CAS# 9002-93-1
Trypsin-EDTA, 0.25%	Thermo Fisher Scientific	Cat# 25200
TWEEN 20	Sigma-Aldrich	Cat# P1379; CAS# 9005-64-5
Wax strips	Veet	N/A

Cell lines	Source	Catalog Number
Human: A375 cell line	ATCC	Cat# CRL-1619; RRID:
Human: SK-MEL-28 cell line	ATCC	Cat# HTB-72; RRID: CVCL_0526
Human: 501Mel cell line	(4)	RRID: CVCL_4633
Human: 888Mel cell line	(4)	RRID: CVCL_4632
Human: M010817 short-term cell culture	URPP Live Tumor Cell	N/A
Human Melanocytes	URPP Human cells	N/A
Mouse Melan-a	Ximbio	Cat# 153599
Mouse: RIM-3 short-term cell culture	(5)	N/A
Mouse: <i>Tyr::Cre^{ERT2}</i> ; B6.Cg-Tg(<i>TyrCre/ERT2</i>)13Bos/J	The Jackson Laboratory	Cat# 012328; RRID: IMSR_JAX:012328
Mouse: <i>R26R-LSL-LacZ</i> ; B6;129S4- <i>Gt(ROSA)26Sor^{tm1Sor}</i> /J	The Jackson Laboratory	Cat# 003309; RRID: IMSR_JAX:003309
Mouse: <i>Smad7^{tm1.1Ink}</i> B6.Cg-Thy1	(6)	MGI: 1100518
Mouse: <i>Tyr::Nras^{Q61K}</i> ; Tg(<i>Tyr NRAS*Q61K</i>)	(7)	MGI: 3768645
Mouse: <i>Ink4a^{-/-}</i> ; <i>Cdkn2a^{tm1Rdp}</i>	(8)	MGI: 1857942
Mouse: <i>Smad4^{tm2.1Cxd}</i> /J	(9)	MGI: 894293

Supplemental References

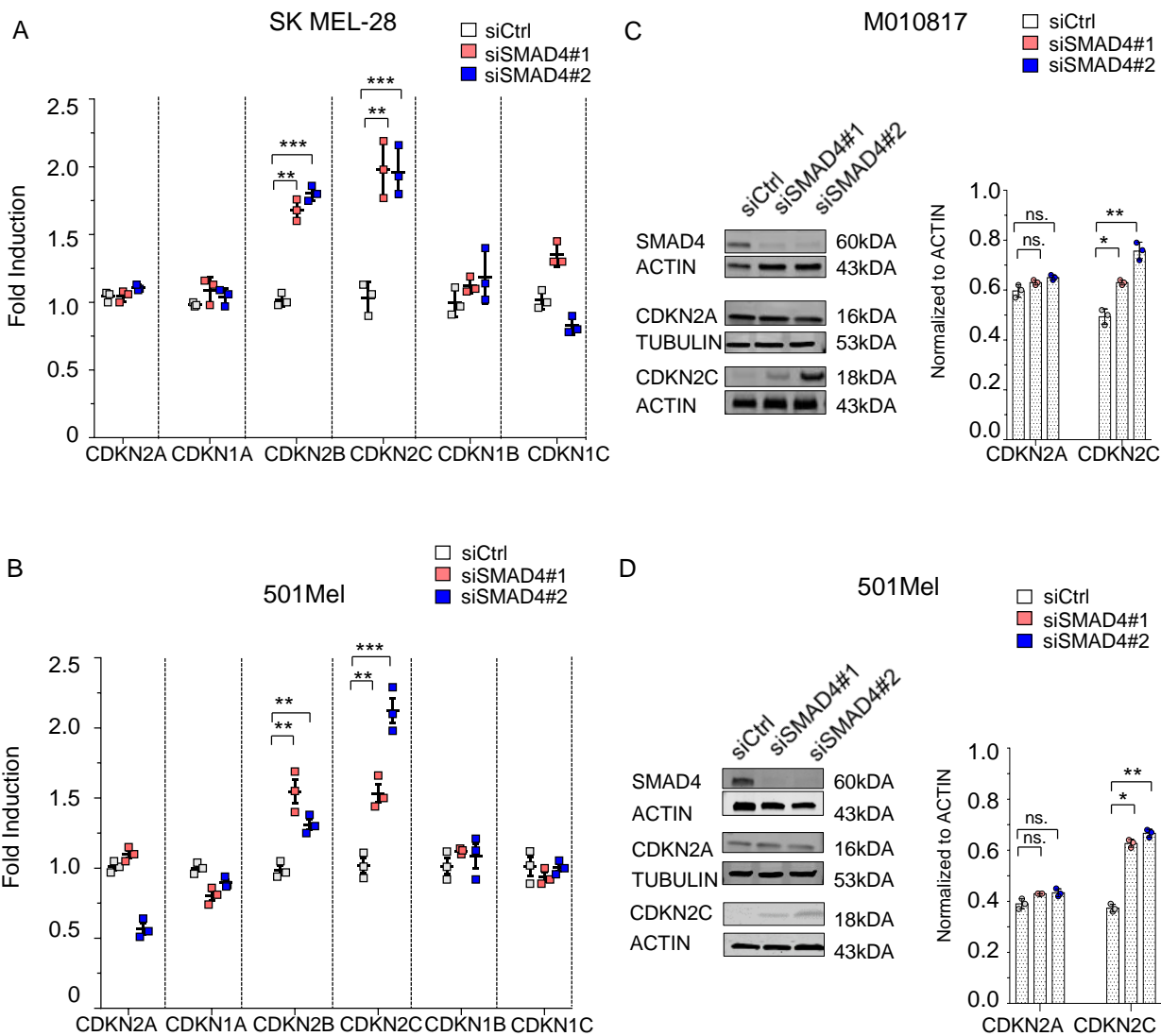
1. Müller-Röver S et al. A comprehensive guide for the accurate classification of murine hair follicles in distinct hair cycle stages. *J. Invest. Dermatol.* 2001;117(1):3–15.
2. Paus R et al. A comprehensive guide for the recognition and classification of distinct stages of hair follicle morphogenesis. *J. Invest. Dermatol.* 1999;113(4):523–532.
3. Raaijmakers MIG et al. A new live-cell biobank workflow efficiently recovers heterogeneous melanoma cells from native biopsies. *Exp. Dermatol.* 2015;24(5):377–380.
4. Rubinfeld B et al. Stabilization of beta-catenin by genetic defects in melanoma cell lines.. *Science* 1997;275(5307):1790–1792.
5. Zingg D et al. The epigenetic modifier EZH2 controls melanoma growth and metastasis through silencing of distinct tumour suppressors. *Nat. Commun.* 2015;6(May 2014):6051.
6. Kleiter I et al. Smad7 in T cells drives T helper 1 responses in multiple sclerosis and experimental autoimmune encephalomyelitis. *Brain* 2010;133(Pt 4):1067–81.
7. Ackermann J et al. Metastasizing melanoma formation caused by expression of activated N-RasQ61K on an INK4a-deficient background. *Cancer Res.* 2005;65(10):4005–11.
8. Serrano M et al. Role of the INK4a locus in tumor suppression and cell mortality. *Cell* 1996;85(1):27–37.
9. Yang X, Li C, Herrera PL, Deng CX. Generation of Smad4/Dpc4 conditional knockout mice. *Genesis* 2002;32(2):80–81.

Supplemental Figure 1



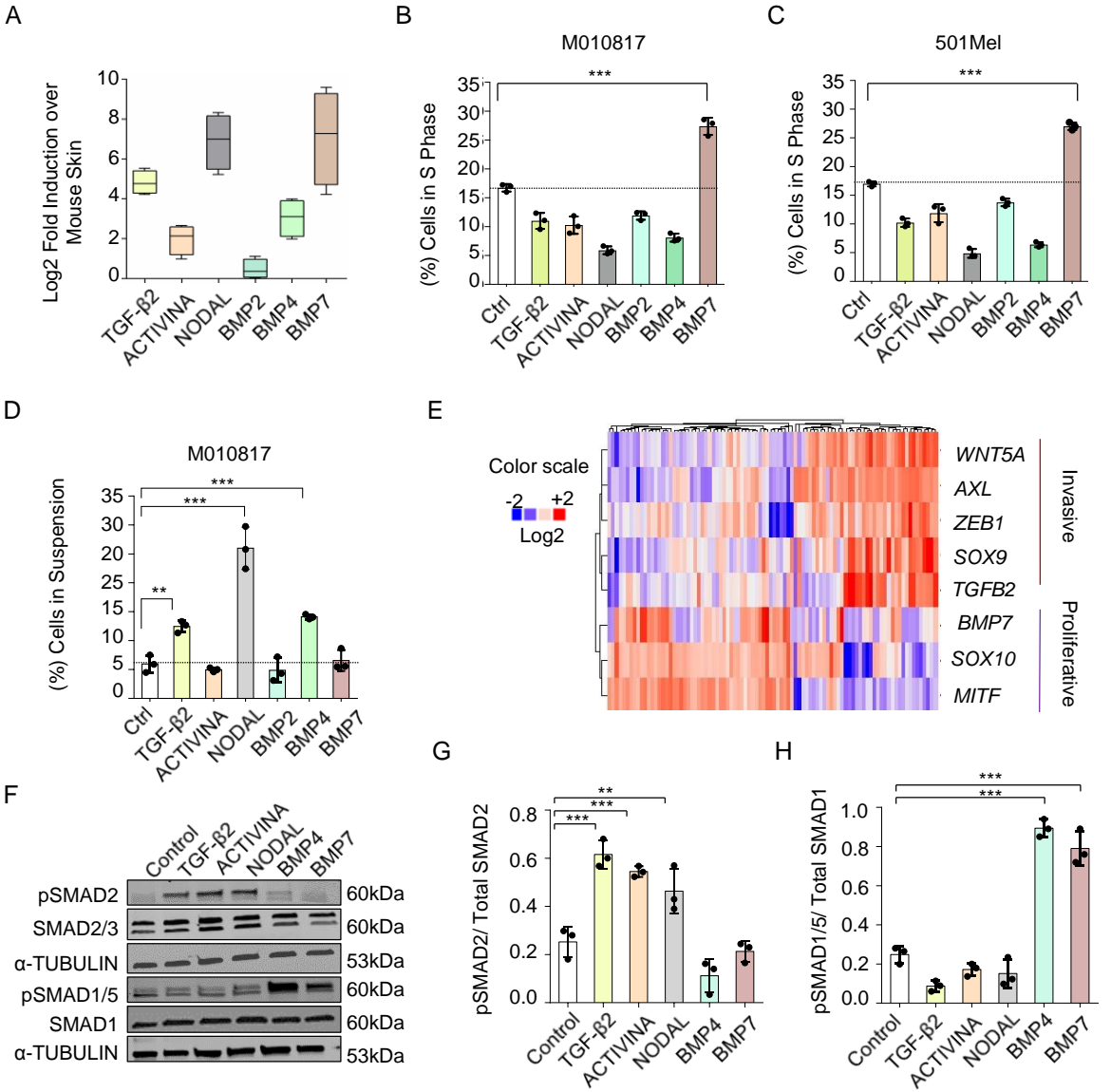
Supplemental Figure 1 Melanocyte-specific deletion of *Smad4* causes hair graying without affecting proliferation rate. (A-C) Breeding and plucking strategy used to analyze the effect of the lack of *Smad4* in *Tyr::Cre^{ERT2}* mice. (D) Quantification of the percentage of recombined hair follicles analyzed by β -Gal expression (cKO, n=7 and 300 hair follicles per animal). (E) Back skin pictures of representative mice at d90 and d128 after plucking. Adult *Smad4^{lox/lox}* *Tyr::Cre^{ERT2}* mice treated with TM by IP injection at the first telogen cycle exhibit white hairs within the plucked region upon hair regrowth. There are no white hairs in similarly treated control mice (F) IF staining for *Smad4*, Dct, and β -Gal protein on back skin sections of control and cKO animals. Bright field images (left panels) reveal reduced pigmentation of cKO hair follicle bulbs in anagen. (G) Percentage of hair follicle bulbs containing β -Gal-positive Dct-expressing melanocytes at the anagen V/IV stage and percentage of β -Gal-positive cells per Dct-expressing hair follicle bulb at the anagen V/IV stage (n=300 hair follicles quantified from three different mice for each genotype). (H,I) Immunostaining for Dct (yellow) and EdU (green) showing proliferation of cells of the melanocytic lineage in the hair follicle bulb (n=3). (J) Appearance of human melanocyte pellets after treatment with siCtrl and siSMAD4, respectively. (K) Percentage of EdU-positive human melanocytes after *SMAD4* knockdown. (L) RT-qPCR analysis of pigmentation-related genes in two human melanocyte cell lines (siCtrl vs siSMAD4#1). Data represented as the mean \pm SD. ns. non-significant, P< 0.01**, P< 0.001***. qPCR results are means \pm SD of three biological replicates. (G,I,K,L) P values calculated with unpaired Student's t-test. P1, postnatal day; d, days; HB, hair bulb.

Supplemental Figure 2



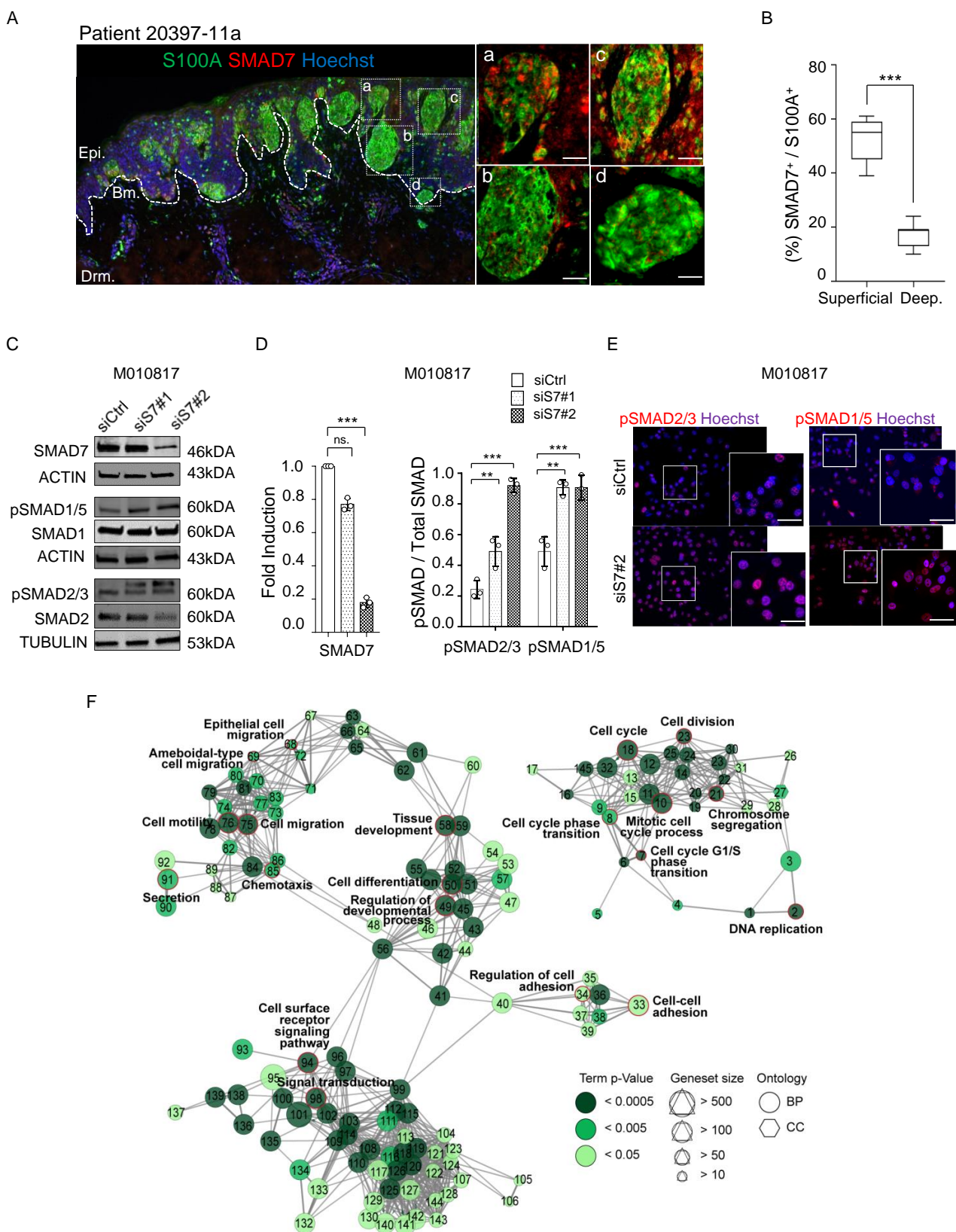
Supplemental Figure 2 Knockdown of SMAD4 alters expression of cell cycle regulators in human and mouse melanoma cell lines. (A,B) RT-qPCR analysis of cell cycle regulators in the indicated human melanoma cell lines. (C,D) Western blot analysis of the cell cycle inhibitors CDKN2A (p16^{INK4a}) and CDKN2C (p18^{INK4c}) in M010817 and 501Mel whole cell extracts treated with siSMAD4. The immunoblots presented were derived from replicate samples run on parallel gels. Data represented as the mean \pm SD. ns. non-significant, P < 0.01**, P < 0.001***. qPCR results are means \pm SD of three biological replicates. (A,B) P values calculated with unpaired Student's t-test.

Supplemental Figure 3



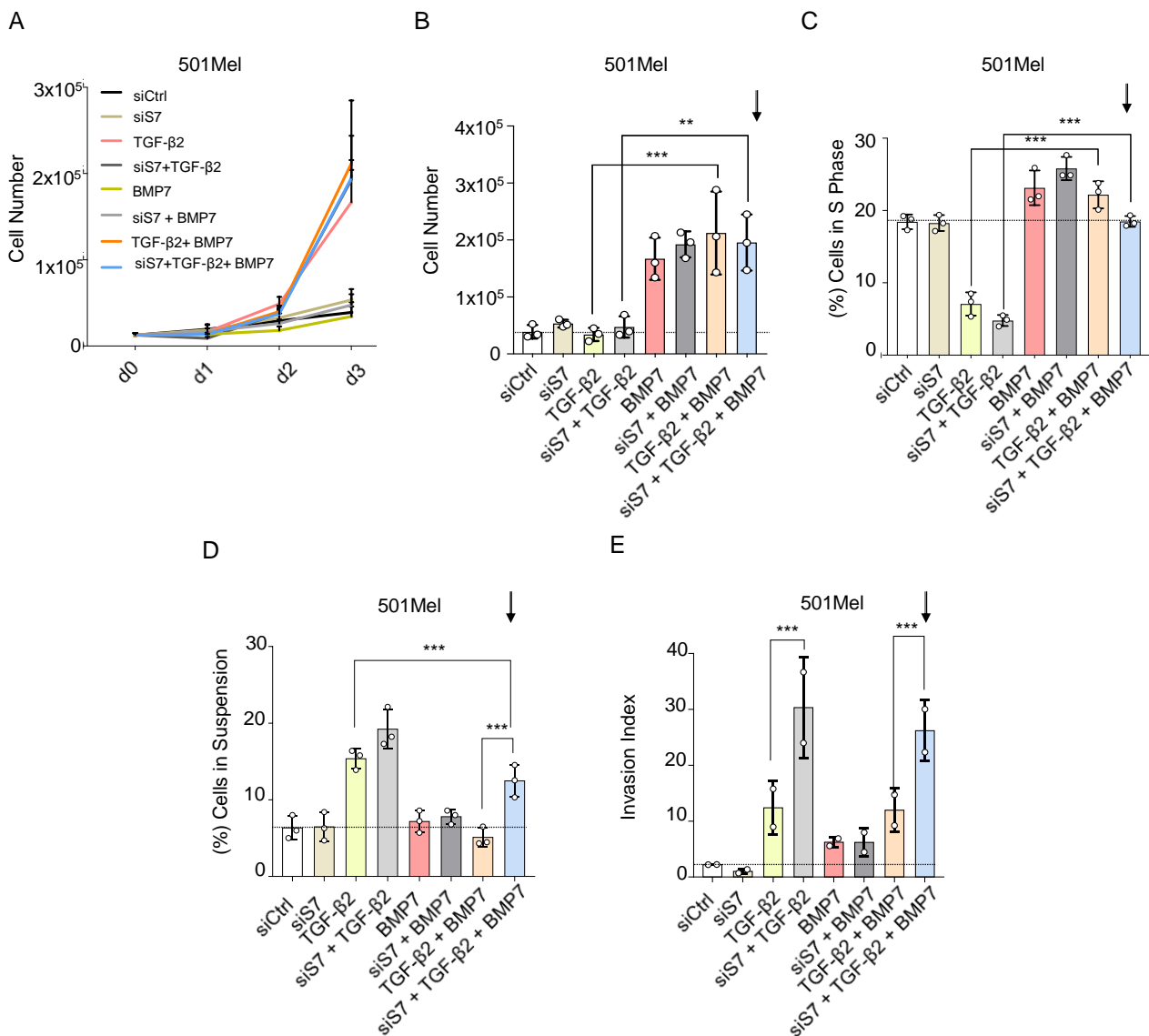
Supplemental Figure 3 BMP7 signaling promotes melanoma cell growth (A) Log2 fold change of ligand mRNAs in primary tumors derived from *Tyr::Nras^{Q61K} Ink4^{-/-}* mice (n=7). (B,C) Cell cycle analysis of M010817 and 501Mel cells exposed to various TGF- β /BMP ligands as described in Supplemental Table 8. Bars represent the percentage of cells distributed in S phase. (D) Quantification of cell-substrate adherence of melanoma cells. (E) Clustering of RNA-seq-based expression data revealing invasive and proliferative cell states in vitro. Samples in the invasive cluster have high expression of the following genes: *WNT5A*, *AXL*, *ZEB1*, *SOX9*, and *TGFB2*. Genes with high expression in the proliferative sample cluster include *BMP7* (*OP1*) and known markers of the melanocyte lineage and melanoma, such as *SOX10* and *MITF*. Correlations of RNA-seq expression data was as follows: *BMP7* and *MITF* $r=0.43$ *** $p<0.001$, *BMP7* and *SOX10* $r=0.39$ *** $p<0.001$, *TGF- β 2* and *ZEB1* $r=0.33$ ** $p<0.01$, *TGF- β 2* and *AXL* $r=0.55$ *** $p<0.001$, *TGF- β 2* and *WNT5A* $r=0.63$, *TGF- β 2* and *SOX9* $r=0.29$, ** $p<0.01$. (F,G) pSMAD2/3 and pSMAD1/5/ were detected in melanoma cells upon ligand treatment by using Western blot analysis. (G,H) Quantification of Western blot analysis, phosphorylation levels of SMAD2/3 and SMAD1/5/8 were determined by using phospho-SMAD specific antibodies and normalized to total SMAD2 and SMAD1/5 levels, respectively. Data are represented as a mean of three independent experiments \pm SD. $P<0.01$ ** , $P<0.001$ ***. P values calculated with one-way ANOVA followed by comparisons to the control group with Bonferroni correction, adjusted $\alpha = 0.05/5 = 0.01$, unpaired Student's t-test (A-D) or Pearson correlation test (E). Data represented as a mean of three independent experiments \pm SD. $P<0.001$ ***. For (H), P values were calculated with unpaired Student's t-test.

Supplemental Figure 4



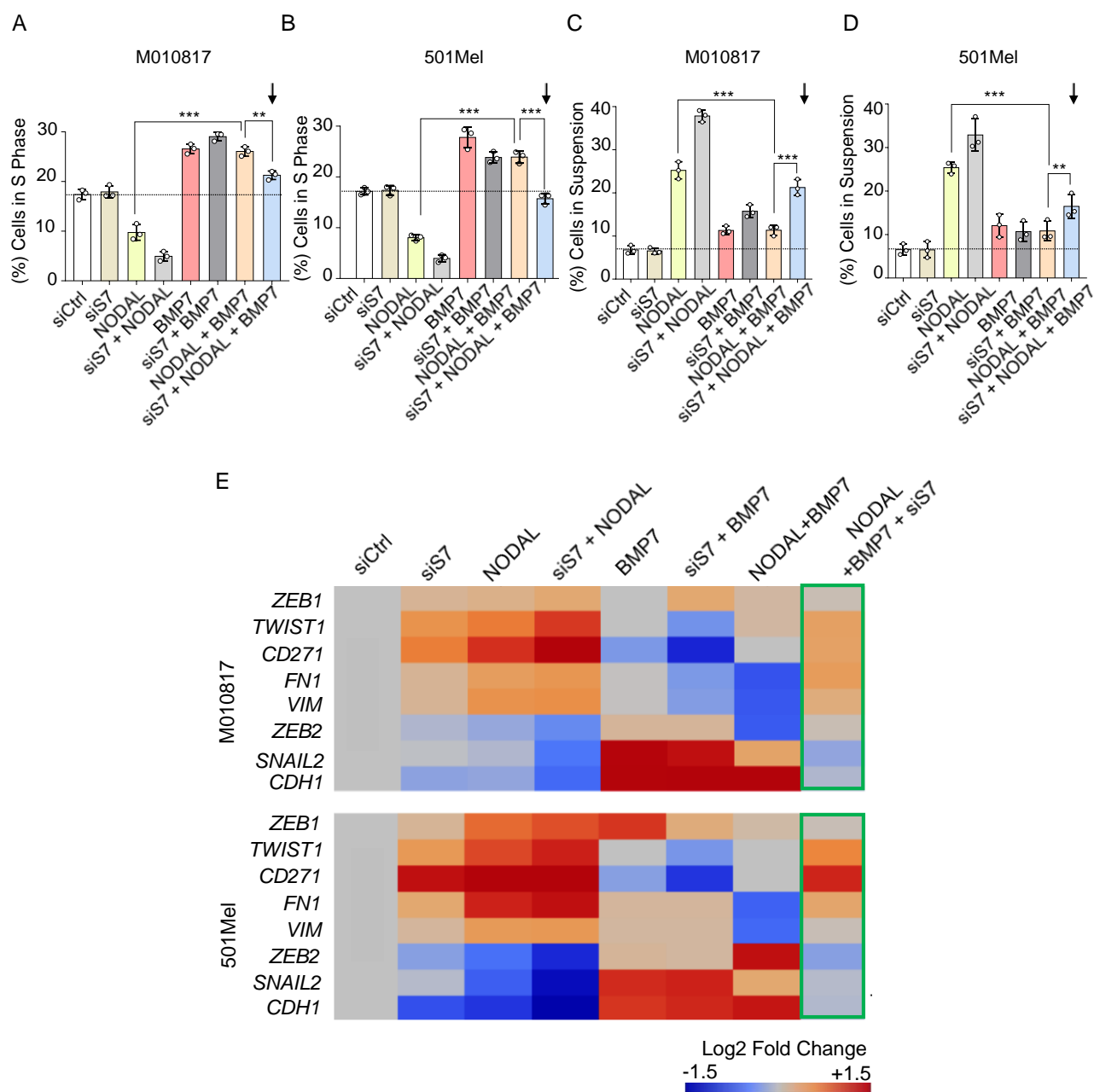
Supplemental Figure 4 Low SMAD7 levels are associated with altered cell adhesion and cell cycle programs in human melanoma cells. (A) An example illustrating co-expression of SMAD7 with S100A in primary melanoma. (B) Quantification of percentage of SMAD7⁺/S100A⁺-double positive cells in superficial and deep sites nodules in human melanoma (n=20 nodules/patient). (C) pSMAD2/3 and pSMAD1/5 were detected in melanoma cells by using Western blot analysis. (D) qRT-PCR analysis for knockdown efficiency for *SMAD7* mRNA expression and quantification of Western blot analysis. SMAD7 levels, phosphorylation levels of SMAD2/3 and SMAD1/5 were determined by normalizing to total SMAD2 and SMAD1/5 levels, respectively. (E) Representative IF images for pSMAD levels. (F) Extended version of gene ontology analysis (Figure 3F) based on differentially regulated genes upon SMAD7 knockdown (each individual node labeled with numbers shows an enriched GO term (P<0.05*) (corrected with Bonferroni step down procedure). BP, biological process; MF, molecular function; CC, cellular component. Individual enriched GO terms are given in Supplemental Table 1. Data are represented as a mean of three independent experiments ± SEM. (B,D) P<0.05*, P<0.01**, P<0.001***. P values calculated with unpaired Student's t-test (E) Data represented as a mean of three independent experiments ± SEM. P<0.001***.

Supplemental Figure 5



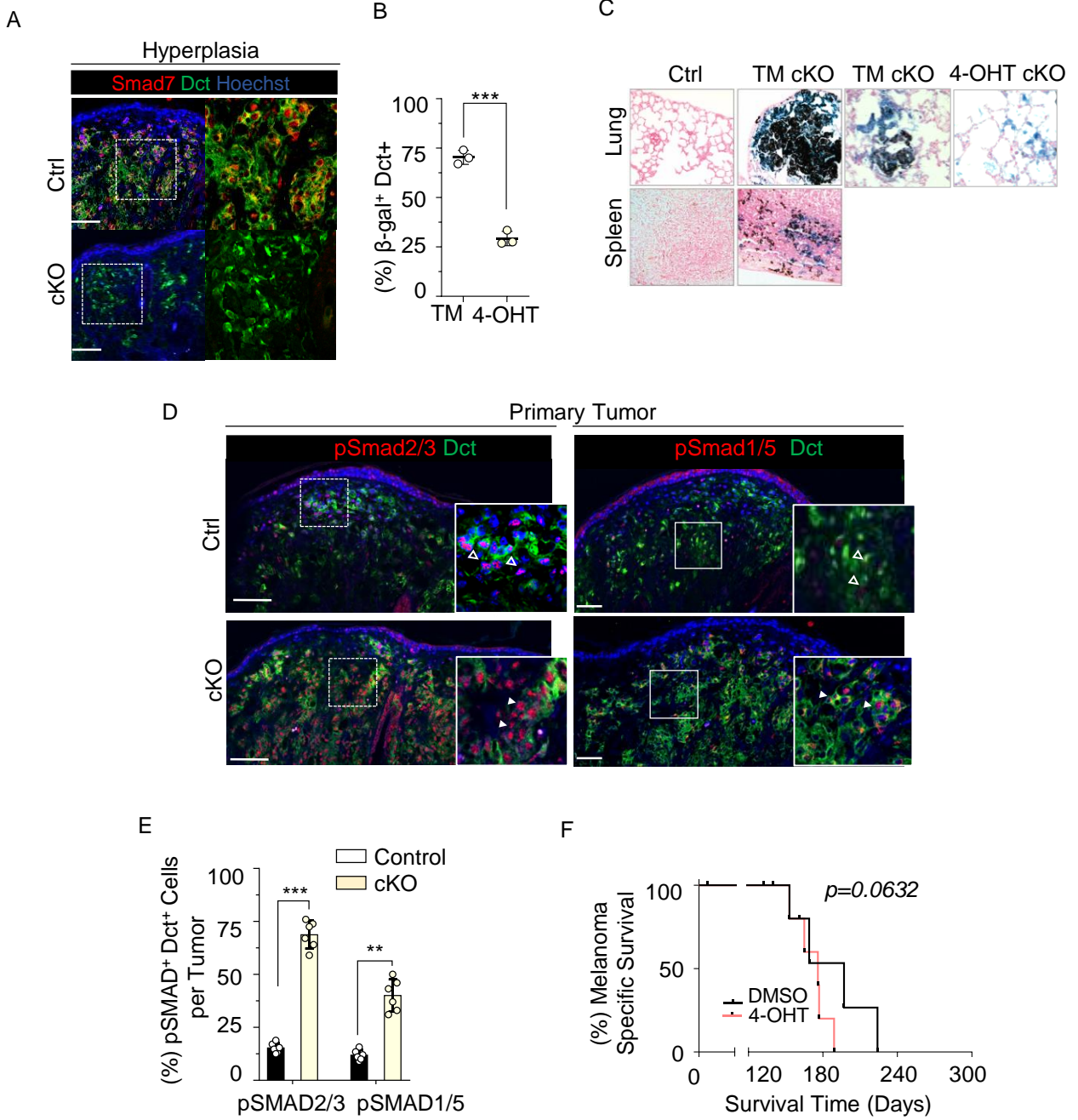
Supplemental Figure 5. Loss of SMAD7 boosts pro-invasive TGF- β signaling in the presence of pro-proliferative BMP7. (A) Growth curves and (B) cell numbers of 501 Mel cells treated as described in Figure 4 (n=1). (C) Quantification of S phase cells measured 3 days post ligand treatment through PI and EdU staining (n=3). (D) Quantification of cell-substrate adherence capacity of 501Mel cells upon various treatments. The percentage of BMP7/TGF- β 2/siSMAD7-treated cells in suspension increased as compared to BMP7/TGF- β 2-treated cells (n=3). (E) Matrigel based invasion assays of siControl and siSmad7-depleted M010817 cells with combinatorial treatments. After invading cells had been counted in five random microscopic fields in each assay, the results were normalized and are presented as an invasion index. Data are represented as a mean of three, two or single independent experiments \pm SD. P values calculated with one-way ANOVA followed by comparisons to the control group with Bonferroni correction (adjusted $\alpha = 0.05/5 = 0.01$). $P < 0.01^{**}$, $P < 0.001^{***}$ (A-E).

Supplemental Figure 6



Supplemental Figure 6. Loss of Smad7 boosts pro-invasive NODAL signaling in the presence of pro-proliferative BMP7. (A,B) Quantification of S phase cells measured 3 days post ligand treatment through PI and EdU staining. Treatment with BMP7 resulted in escape of cells from the NODAL-mediated cell cycle arrest and increase in the proliferation rate. SMAD7 knockdown along with BMP7/NODAL treatment results in decreased percentage of cells in S phase as compared to BMP7/NODAL treatment. (C,D) Quantification of cell-substrate adherence capacity of human melanoma cells upon various treatments. (E) Heat map shows qRT-PCR analysis for selected EMT genes under ligand treatments with two biological and three technical replicates. Data represented as a mean \pm SD. P values calculated with one-way ANOVA followed by comparisons with the control group with Bonferroni correction (adjusted $\alpha = 0.05/5 = 0.01$). $P < 0.01^{**}$, $P < 0.001^{***}$ (A-E).

Supplemental Figure 7



Supplemental Figure 7. Reduced Smad7 expression promotes massive metastatic spread of melanoma *in vivo*. (A) Immunofluorescent staining for Smad7 and Dct on back skin sections at 6 months of age. Melanocytic cells are recombined and show decreased levels of Smad7 (n=6). (B) Quantification of the recombination efficiency by analyzing the percentage of Dct/ β -Gal⁺ double-positive cells upon intraperitoneal injection or local application of 4-hydroxytamoxifen (4-OHT) to the back skin of 3-week-old mice (n=3). (C) Representative hematoxylin and eosin staining of lung and spleen sections of control and cKO mice at the day of sacrifice. X-Gal staining (blue) illustrates presence of recombined metastatic cells in distant organs. (D) Immunofluorescent staining for pSmad2/3, pSmad1/5 and Dct of primary tumors at 6 months (n=6). Control and cKO primary tumors were quantified for active TGF- β signaling by detecting the nuclear localization of pSmad2/3 or pSmad1/5 (n=6). (E) Quantification of active TGF- β signaling by quantifying the number of melanocytic Dct⁺ cells displaying nuclear localization of pSmad2/3 and pSmad1/5/8, respectively, in primary tumors at 6 months (n=6). (F) Kaplan–Meier curves comparing overall survival between 4-OHT treated animals and control animals (n=8). Data represented as a mean of three independent experiments \pm SD. P values calculated with unpaired Student's t-test (B), log-rank (Mantel–Cox) test (F). P < 0.05*, P < 0.01**, P < 0.001***. Scale Bars: 50 μ m (A,D).